A CONSTITUTIVE MODEL FOR CREEP LIFETIME OF PBO BRAIDED CORD

W. J. Sterling
NASA Goddard Space Flight Center's Wallops Flight Facility
Wallops Island, VA 23337

Abstract

A constitutive model to describe the creep lifetime of PBO braided cord has been developed and fit to laboratory data. The model follows an approach proposed for *p*-aramid cord in similar applications, and has a Boltzman-type representation that arises from consideration of the failure phenomenon mechanism. The data were obtained using a hydraulic-type universal testing machine, and were analyzed according to Weibull statistics using commercially-available software. The application of concern to the author is NASA's Ultra-Long Duration Balloon and other gossamer spacecraft, but the motivations for the related *p*-aramid works suggest broader interest.

Background

NASA's Ultra-Long Duration Balloon (ULDB) design presently uses braided cord made of PBO (Zylon® HM) fibers in non-redundant load tendons. This material was chosen on the basis of unique properties that enable the balloon design; however, it also presents significant challenges. Other works discuss most of these challenges [1-4]. The focus of this paper is on the tendon lifetime under anticipated flight conditions, which are approximated as steady-load, or creep.

Creep rupture is the phenomenon wherein a material fails after finite time of static loading below the ultimate tensile strength as measured under dynamic tensile conditions. It is essentially a physical deterioration of strength while under creep conditions. The time from initial loading until material failure is called the creep lifetime. For applications requiring a steady, or near-steady, load for a given duration at extremely low failure probability, mean field approaches such as averaging are excluded because the critical events occur in the low-strength extremities of the material strength probability distribution tail [5-7]. Alternately, the critical events can occur in the high-stress extremities of the structural load probability distribution tail, but the focus here is on the material properties.

Fortunately, the literature discusses that creep lifetime for *p*-aramid (Kevlar®), a cousin to PBO, may be represented by a mechanistic mathematical model of the material failure phenomenon. Although the failure mechanism(s) may be different for PBO, the mathematical form that arises from the mechanism favored herein is generally adaptable to others.

Constitutive Model Development

Creep failure of fiber bundles is believed to occur as the result of accumulating fiber breaks that eventually manifest as rapid local deformation leading to a catastrophic event [5,8]. The local deformation may cause rapidly increasing strain (i.e., tertiary creep), that is not evident on the macroscopic scale. In materials such as high-modulus polymer and glass fibers, observable creep is very small even at failure.

The failure time variability of individual fibers subjected to the same stress is typically very high [7,9,10], but is also typically well-represented by Weibull statistics [5,11]. The variability is likely due to random imperfections arising from manufacturing and processing which may be especially prevalent in braided cords. The stress on an individual fiber falls to zero at the instant of failure, but may return as the fiber re-engages via friction with its neighbors. Concomitant with a fiber failure is the over-stressing of its neighbors through shear transfer. When a statistically significant collection of failures occur within a localized region, or when local collections of failures merge, a cascade of failure events ensues and leads rapidly to bundle failure. The level of yarn failure that may lead to rope breakage may be less than 1% [8].

According to statistical bundle theory [12], the static strength of a bundle of fibers is less than the average strength of the individual fibers, and under the same static stress the time to failure of a bundle is less than for an average fiber. The static failure stress of ropes tends to decrease as the cross-sectional area (number of fibers) increases, becoming asymptotically constant [6]. Therefore, the logical way to represent lifetime data is to normalize the applied stress by the tensile strength [13], and that representation has been widely used [6,7,9-11, 14] even though the molecular mechanisms for short-term and long-term failure may be significantly different [14].

There are two basic theories for stress rupture in polymers, molecular processes and fracture mechanics. Zhurkov developed the most widely-used molecular model [6], which describes the failure for polymers below their glass transition temperature as due to mechano-chemical scission of polymer backbone bonds [15-16].

The scission energy comes from two sources, heat and stress, which implies that at higher temperature less stress is needed for rupture, and further suggests that creep lifetime increases as temperature decreases. Recent publications strongly support the Zhurkov theory [14,17] and mention that this theory has been independently developed by others [10,17].

On the other hand, fracture mechanics theory suggests the rupture may be due to weak intercrystalline affinity [18-21], agglomeration of amorphous regions [22-24], or some combination thereof [9,18]. However, these broad mechanisms are unlikely to be mutually exclusive, and they lead to similar mathematical representations differing only in the rate-controlling step of many kinetic phenomena [6,10]. Because the Zhurkov theory is more widely-accepted and has a well-developed basis in physics, it will be highlighted here.

Not surprisingly, the Zhurkov model proposes a Boltzmann-type mechanism whereby the failure time (t_b) is presented as an exponential function of barrier energy,

$$t_b = t_o \exp[(U - B\sigma)/kT], \quad (1)$$

where k is the Boltzmann constant, T is the absolute temperature, U is the activation (or bond dissociation) energy, and B relates the applied stress, σ, to the bond stress. As suggested above, the applied creep stress will be normalized by the dynamic tensile failure stress in the analysis. The pre-exponential factor, t_o, has been described as the characteristic time for atomic vibrations [15-16] and the bond thermal oscillation period [25], and its value has been estimated to be 10^{-11} to 10^{-13} s [17,25].

Zhurkov's representation can be rearranged to

$$ln\ t_b = \alpha + \kappa\sigma \quad (2)$$

where $\alpha = ln\ t_o + U/kT$ and $\kappa = -B/kT$. We will adopt the mechanistic model expressed in Eq.2, and utilize α and κ as fitting parameters, noting that although we are not working directly with the fundamental physical quantities, we have maintained contact with them, and given the appropriate data, we could determine them. Since Eq.2 has such a common and general form, it should not be surprising to discover that it could also be used to represent alternate mechanistic models. A landmark study on stress-rupture of *p*-aramid [11] applied the form of Eq.2, although the authors apparently did so without knowledge of the Zhurkov theory.

Statistical Representation of Data

Although often neglected in the engineering community, it is widely documented that the Normal distribution, and the accompanying use of the mean and standard deviation as characterizing metrics, is not likely to be appropriate for describing the capabilities of materials used in strength- or lifetime-critical applications [e.g., 3,26-28]. It is more appropriate in these cases to use extreme value distributions such as Weibull and Log-Normal because these reduce exposure to unreasonable representations such as zero or negative strength and generally match the data shape distribution better.

The Weibull distribution will not be discussed further here, except to state its form,

$$P(t_b) = 1 - \exp[-(t_b/\eta)^{\beta}], \quad (3)$$

where t_b is the time to failure, P is the failure probability, and the fitting parameters are η, the distribution scale, and β, the distribution shape [11].

The next step in the development is to bring the statistical representation of the failure data together with the mechanistic failure model. For each creep stress level, the probability density function is fitted to the data using commercially-available software [29,30]. The variation in the fitting parameters with stress is then represented by the mechanistic model for the failure phenomenon [6,11,14,25].

When the fitting parameters are expressed in terms of the mechanistic failure model,

$$\eta = \alpha_\eta \exp(-\kappa_\eta f) \quad (4)$$

and

$$\beta = \alpha_\beta \exp(-\kappa_\beta f), \quad (5)$$

where f is the ratio of creep stress to ultimate tensile stress. The failure time is then seen to be predictable for desired stress and failure probability levels. When the natural logarithm of η is plotted versus f, κ_η arises as the negative slope and α_η is exp(intercept). The parameters for β are analogously determined.

Laboratory Procedure

Creep and tensile experiments were performed using an Instron 8505 hydraulically-driven universal testing machine (UTM). Specimens were fabricated from 48,000 denier braided cord by tying Brummel splices in each end, and were attached to the UTM via load pins. The ultimate tensile strength (UTS) in dynamic loading was determined via tests at constant strain rates over 0.015-19 %/min. Creep lifetime measurements were made at several high fractions of the UTS. Lower load levels require considerably longer test times, which are more likely to exceed the reliable conduct of this test type. Tests at lower fractions of UTS are being pursued. Further details about the PBO braided cord material and test methods have been documented elsewhere [2,4].

Results

The creep lifetime data are presented in Figure 1 on Weibull axes. In an analogous paradigm to logarithmic axes, data which fit the Weibull distribution well appear

linear when plotted on Weibull axes. The software used to generate this plot and fit the data to the Weibull distribution [29,30] showed good fitting metrics for the three samples. Table 1 gives the Weibull fit parameters for each load level. These parameters are then plotted on semi-log axes according to Eqs. 4-5 in Figs. 2-3. Linear least squares fitting for $ln\eta$ (Fig. 2, Eq. 4) yields $ln\alpha_\eta$=44.05, κ_η=0.43, and R^2=0.9997. The linear least squares fitting parameters for $ln\beta$ (Fig. 3, Eq. 5) are $ln\alpha_\beta$=2.12, κ_β=0.03, and R^2=0.9998. It is evident that the data support the theory.

The goal of this work is to provide a guide for designers and engineers who intend to use this material in a static, or near-static, manner. Figure 4 provides such advice as a plot of lifetime to be anticipated as a function of loading and acceptable failure probability. The interpretation of Figure 4 is that for an application requiring approximately one month duration ($ln t_b \approx 15$) with acceptable failure probability of 1% (P=0.01), the maximum loading should be 60% (f=0.6) of the cord ultimate tensile strength. Of course, interpretations beyond the available data should be done cautiously. Analysis of additional lifetime data from experiments at lower creep stress levels is underway.

Summary

A Boltzman-type phenomenological model for creep rupture, when coupled with a Weibull statistical analysis of laboratory data, provides a useful constitutive representation for the creep lifetime of braided PBO cord. This model will be useful to NASA's ULDB project, and also perhaps to other aerospace and civil engineering applications.

Acknowledgements

Ron Allred of Adherent Technologies in Albuquerque made helpful suggestions. Walt Thomas of NASA-Goddard was helpful with the Weibull statistical analysis. The data were obtained by technicians in NASA's Balloon R&D Laboratory. This work was funded by NASA's Balloon Program Office.

References

1. Sterling, W.J., *submitted*, American Institute for Aeronautics and Astronautics, *Aerodynamic Decelerator Systems and Balloon Systems Conference*, Williamsburg, VA, 2007.
2. Sterling, W.J., and Fairbrother, D.A., Paper No. 2004-1658, American Institute for Aeronautics and Astronautics, *45th Structures, Structural Dynamics, and Materials Conference*, Palm Springs, 2004.
3. Schur, W.W., Green, C.B., and Sterling, W.J., Paper No. 2003-6778, American Institute for Aeronautics and Astronautics, *3rd Aviation Technology, Integration, and Operations Conference*, Denver, 2003.
4. Sterling, W.J., Paper No. 2003-6777, American Institute for Aeronautics and Astronautics, *3rd Aviation Technology, Integration, and Operations Conference*, Denver, 2003.
5. Phoenix, S.L., *Composite Structures*, **48**, 19, 2000.
6. Burgoyne, C.J., and Guimarães, G.B., *Proc. International Conf. Advanced Composite Materials in Bridges and Structures (ACMBS)*, M.M. El-Badry (ed.), Canadian Society for Civil Engineering, Montreal, 1996.
7. Boone, J.D., Paper No. 75-1363, American Institute for Aeronautics and Astronautics, *5th Aerodynamic Decelerator Systems Conference*, Albuquerque, 1975.
8. Burgoyne, C.J., and Mills, P.D., *Proc. International Conf. Advanced Composite Materials in Bridges and Structures (ACMBS)*, M.M. El-Badry (ed.), Canadian Society for Civil Engineering, Montreal, 1996.
9. Lafitte, M.H., and Bunsell, A.R., *Polym. Eng. Sci.*, **25** (3), 182, 1985.
10. Wagner, H.D., Schwartz, P., and Phoenix, S.L., *J. Materials Science*, **21**, 1868, 1986.
11. Chiao, T.T., Wells, J.E., Moore, R.L., and Hamstad, M.A., *Composite Materials: Testing and Design (3rd Conference), ASTM STP 546*, American Society for Testing and Materials, 209, 1974.
12. Phoenix, S.L., *Int'l. J. Fracture*, **14** (3), 327, 1978.
13. Chambers, J.J., and Burgoyne, C.J., *J. Materials Science*, **25**, 3723, 1990.
14. Wu, H.F., Phoenix, S.L., and Schwartz, P., *J. Materials Science*, **23**, 1851, 1988.
15. Zhurkov, S.N., and Korsukov, V.E., *J. Polym. Sci.*, **12**, 385, 1974.
16. Zhurkov, S.N., and Kuksenko, V.S., *Int'l. J. Fracture*, **11** (4), 629,1975.
17. vonSchmeling, H.H.K.B., *Physics of the Solid State*, **47** (5), 934, 2005.
18. Ericksen, R.H., *Polymer*, **26**, 733, 1985.
19. Kitigawa, T., and Yabuki, K., *J. Polym. Sci. B: Polym. Phys.*, **38**, 2901, 2000.
20. Kitigawa, T., and Yabuki, K., *J. Polym. Sci. B: Polym. Phys.*, **38**, 2937, 2000.
21. Rao, Y., Sakuda, M., and Farris, R.J., *Korea Polymer J.*, **6** (1), 91, 1998.

22. Ohta, Y., Kaji, A., Sugiyama, H., and Yasuda, H., *J. Appl. Polym. Sci.*, **81**, 312, 2001.

23. Yeh, W.Y., and Young, R.J., *Polymer*, **40**, 857, 1998.

24. Hodson, J., Pruneda, C.O., Kershaw, R.P., and Morgan, R.J., *Composites Technology Review*, **5** (4), 115, 1983.

25. Chiao, C.C., Sherry, R.J., and Hetherington, N.W., *J. Composite Materials*, **1**, 79, 1977.

26. Meeker, W.Q., and Escobar, L.A., *Statistical Methods for Reliability Data*, Wiley-Interscience, New York, 1998.

27. Annis, C.E., Paper No. 2003-1572, American Institute for Aeronautics and Astronautics, *5th Non-Deterministic Approaches Forum*, Norfolk, 2003.

28. Box, G.E.P, Hunter, W.G., and Hunter, J.S., *Statistics for Experimenters*, John Wiley & Sons, New York, 1978.

29. Abernethy, R.B., *The New Weibull Handbook*, 4th ed., available through the Society of Automotive Engineers (SAE International), the American Society of Mechanical Engineering (ASME), and www.bobabernethy.com, 2000.

30. Fulton, W., *SuperSMITH*™ software, v. 4.0WH, available via www.weibullnews.com or Ref.29, 2004.

Key Words

Braided cord, creep lifetime, creep rupture, Kevlar®, PBO, *p*-aramid, ULDB, Zylon®.

Load (% of UTS)	Eta (η), secs	Beta (β)
90	258	0.493
85	2,331	0.579
80	18,539	0.675

Table 1. Weibull fit parameters (Eq. 3) for creep lifetime data shown in Fig. 1.

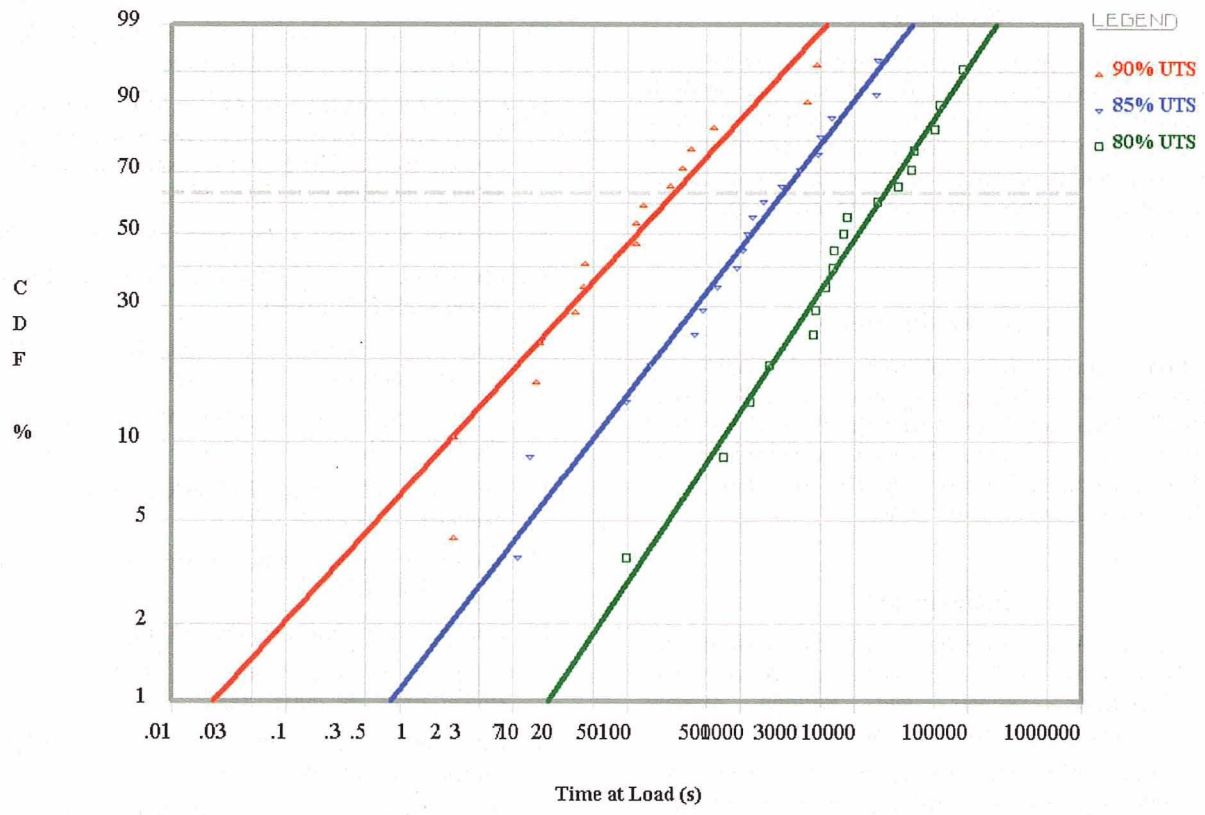

Figure 1. Creep lifetime data presented on Weibull axes. CDF = cumulative distribution function. The heavy broken grid line at CDF = 63.2% corresponds to η for all Weibulls.

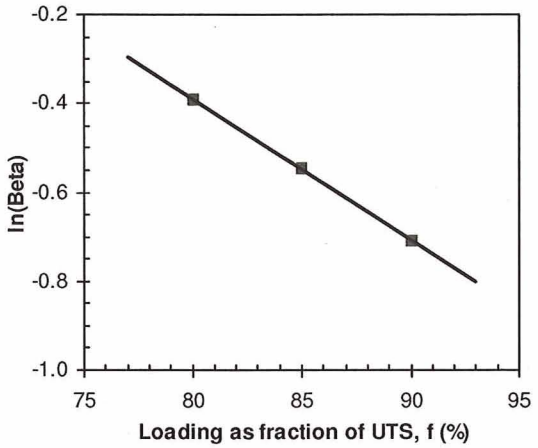

Figure 2. Weibull scale parameter plotted according to failure model.

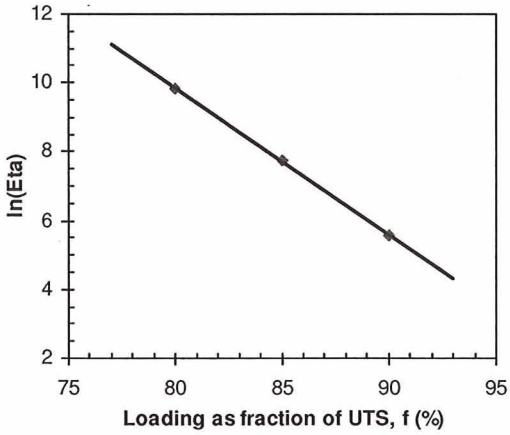

Figure 3. Weibull shape parameter plotted according to failure model.

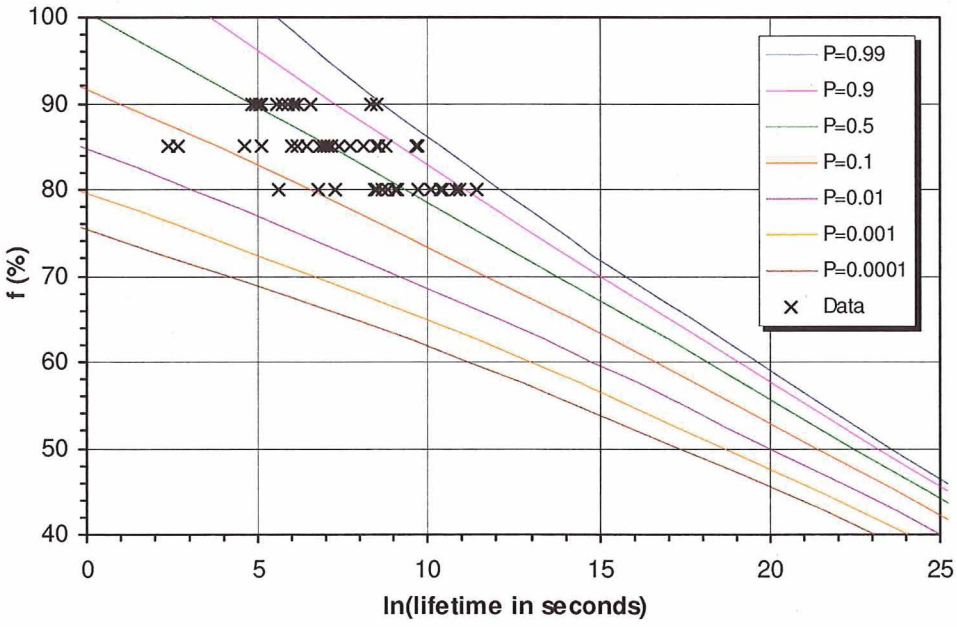

Figure 4. Lifetime probability plot showing laboratory data.